Electronic Structure and Valence-Bond Band Structure of Cuprate Superconducting Materials

Yuejin Guo; Jean-Marc Langlois; William A. Goddard

Science, New Series, Vol. 239, No. 4842 (Feb. 19, 1988), 896-899.

Stable URL:
http://links.jstor.org/sici?sici=0036-8075%2819880219%293%3A239%3A4842%3C896%3AESAVBS%3E2.0.CO%3B2-2

Science is currently published by American Association for the Advancement of Science.

Reports

Electronic Structure and Valence-Bond Band Structure of Cuprate Superconducting Materials

YUEJIN GUO, JEAN-MARC LANGLOIS, WILLIAM A. GODDARD III

From ab initio calculations on various clusters representing the $La_{2-x}Sr_xCu_1O_4$ and $Y_1Ba_2Cu_3O_7$ classes of high-temperature superconductors, it is shown that (i) all copper sites have a Cu^{II} (d^9) oxidation state with one unpaired spin that is coupled antiferromagnetically to the spins of adjacent Cu^{II} sites; (ii) oxidation beyond the cupric (Cu^{II}) state leads not to Cu^{III} but rather to oxidized oxygen atoms, with an oxygen $p\pi$ hole bridging two Cu^{II} sites; (iii) the oxygen $p\pi$ hole at these oxidized sites is ferromagnetically coupled to the adjacent Cu^{II} d electrons despite the fact that this is opposed by the direct dd exchange; and (iv) the hopping of these oxygen $p\pi$ holes (in CuO sheets or chains) from site to site is responsible for the conductivity in these systems (*N*-electron band structures are reported for the migration of these localized charges).

TO ELUCIDATE THE MECHANISM RESPONSIBLE for high-temperature superconductivity in various cuprates, we carried out first principles quantum chemical calculations on models of the $La_{2-x}Ba_xCu_1O_4$ (denoted 2-1-4) and the $Y_1Ba_2Cu_3O_7$ (denoted 1-2-3) classes of systems (*1, 2*). The resulting wavefunctions indicate that electrical conduction in these systems is dominated by hopping of oxygen $p\pi$ holes from site to site in the CuO sheets and chains, and we report the band structures based on these valence-bond localized states. In addition, there are important magnetic couplings between spins on adjacent copper atoms and between the conduction electrons (oxygen $p\pi$ holes) and the copper spins that are critical in the superconductivity.

Electronic structure of the reduced (Cu^{II}) system. The electronic wavefunctions were calculated with the generalized valence bond (GVB), Hartree-Fock (HF), or configuration interaction (CI) methods (*3*). Calculations (*4–7*) were carried out on finite clusters as indicated in Fig. 1. In each case we included explicitly all electrons on the atoms shown plus the point charge approximation to all other ions within about 8 Å. The sphere size was adjusted slightly (up to 0.2 Å) so that balanced sets of ions were included, with the outer boundary always being oxygen. The charge on the outer layer was scaled so that the whole cluster is neutral. The number of explicit electrons corresponds to having O^{2-} and Cu^{2+} or Cu^{3+} at each atom shown. The wavefunctions were calculated self-consistently for each state.

We find in all cases (four-, five-, and six-coordinate) that the optimum wavefunctions have nine electrons in d orbitals on each copper, with the singly occupied orbital pointing at the four short bonds. For example, the singly occupied d-like orbitals for the 1-2-3 chain are shown in Fig. 2, a and b (cluster Cu_3O_{10}). The total population in d orbitals on the three copper sites is $d^{9.15}$, $d^{9.17}$, and $d^{9.15}$. The electrons formally considered on O^{2-} are partially shared with the copper so that the total charge on the copper is +0.41, +0.23, and +0.41 for this cluster (rather than +2, +2, and +2). Similar results are obtained for the 1-2-3 stub (Cu_3O_{12}), where the d populations are $d^{9.05}$, $d^{9.17}$, and $d^{9.05}$ (total charges 0.44, 0.45, and 0.44). For the 2-1-4 system (Cu_2O_{11}), the d populations are $d^{9.11}$ and $d^{9.11}$ (total charges −0.23 and −0.23).

With one singly occupied orbital per copper, the Cu_2 systems lead to two low-lying spin states ($S = 0$ and $S = 1$), and the Cu_3 systems lead to three low-lying states ($S = 1/2$, $S = 1/2$, and $S = 3/2$). We solved self-consistently for each of these states using the GVB wavefunction and fitted the resulting energies to a Heisenberg spin Hamiltonian,

$$H = -\sum_{i<j} 2J_{ij}\mathbf{S}_i \cdot \mathbf{S}_j \qquad (1)$$

For the Cu_2 cases, the singlet is lower because the orbitals overlap slightly ($\sigma = 0.05$), leading to an "antiferromagnetic" exchange integral J, where $J = -205$ K for the Cu_2O_{11} sheet and $J = -244$ K for the Cu_2O_7 chain. From the Cu_3 systems we find that $|J_{dd}| < 0.1$ K for second nearest neighbors ($\sigma = 0.0006$). In one and two dimensions, a system described by Eq. 1 with negative J leads to an ordering (Néel) temperature of $T_N = 0$ K (*8*). Hence, long-range order is not expected at finite T. Experimental evidence on La_2CuO_{4-y} suggests that there are strong short-range couplings; however, evidence for long-range order is conflicting, with one report of $T_N = 220$ K (*9*). For the Cu_3 stub (Cu_3O_{12}), the $d_{z^2-y^2}$ orbitals of the center (chain) copper are orthogonal to the $d_{x^2-y^2}$ orbitals of the top and bottom (sheet) copper sites, leading to weak ferromagnetic coupling ($J_{dd} = +11$ K).

Although each system has an array of singly occupied copper d orbitals, it does not lead to electrical conduction. The reason is that the charge transfer state ($Cu^{II} \cdots Cu^{II} \rightarrow Cu^{I} \cdots Cu^{III}$) is very high in energy (about 10 eV for the Cu_2O_{11} cluster). In band language, the system has a large Hubbard U parameter (one center electron-electron repulsion), leading to an exceedingly narrow band.

The oxidized ("Cu^{III}") system. The cuprates exhibiting superconductivity all are oxidized further than Cu^{2+}. Assuming no oxygen vacancies, the copper of $La_{1.85}Sr_{0.15}Cu_1O_4$ is 15 percent oxidized, and the copper of $Y_1Ba_2Cu_3O_7$ is 33 percent oxidized. However, other systems (for example, $La_4BaCu_5O_{13}$ and $La_5SrCu_6O_{15}$) have similar levels of oxidation but do not exhibit superconductivity (down to 5 K) (*10*). For all systems discussed here we find that oxidation of the Cu^{II} (d^9) leads not to Cu^{III} (d^8)

$$O\text{–}Cu^{II}\text{–}O\text{–}Cu^{II}\text{–}O \rightarrow O\text{–}Cu^{III}\text{–}O\text{–}Cu^{II}\text{–}O \qquad (2)$$

but rather to oxidation out of an oxygen $p\pi$ singly occupied orbital (see Fig. 2c) located between two Cu^{II} sites,

$$O\text{–}Cu^{II}\text{–}O\text{–}Cu^{II}\text{–}O \rightarrow O\text{–}Cu^{II}\text{–}O^{+}\text{–}Cu^{II}\text{–}O \qquad (3)$$

Thus, in the oxidized systems, all coppers have the Cu^{II} (d^9) oxidation state, but each oxidation leads to a singly occupied oxygen $p\pi$ orbital that is spin-coupled to the various singly occupied copper d orbitals. We will show below that hopping of such oxygen $p\pi$ holes from site to site leads to electrical conduction if the hole is on the proper oxygen.

The $La_{2-x}Sr_xCu_1O_4$ system has two-dimensional sheets of copper and oxygen as in

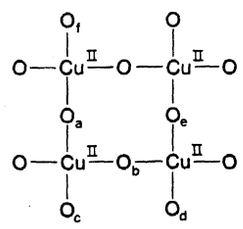

I

where each Cu-O bond is 1.89 Å. In addition, there are apex oxygens 2.40 Å above and below each copper. For $x = 0$, we find that oxidation of the in-plane (sheet) oxygen

Arthur Amos Noyes Laboratory of Chemical Physics, California Institute of Technology, Pasadena, CA 91125.

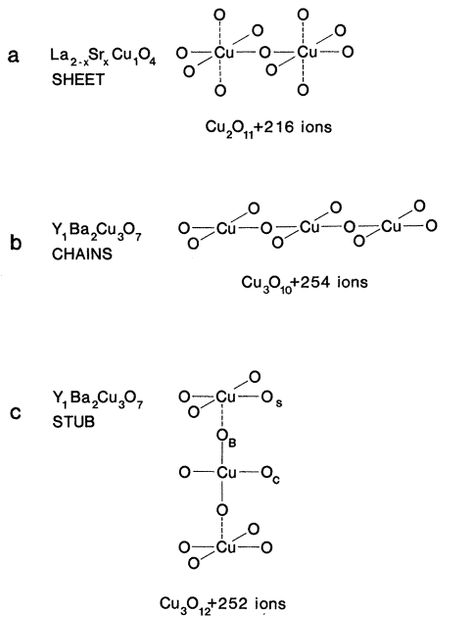

Fig. 1. Clusters used in GVB calculations. The array of point charges extends out to ~8 Å from each copper (adjusted so that the outer shells are oxygens). The charges on the point charges are the nominal values (O^{2-}, Y^{3+}, Ba^{2+}) except for Cu where $Cu^{+2.15}$ was used for $La_{1.85}Sr_{0.15}CuO_4$ and $Cu^{+2.33}$ was used for $Y_1Ba_2Cu_3O_7$. In addition, for $La_{2-x}Sr_xCuO_4$ an averaged charge $Z = 3 - \frac{1}{2}x$ was used for the LaSr system. The number of explicit electrons was based on the nominal charges [for example, $(Cu_3O_{10})^{14-}$ with three Cu^{II}]. In all calculations, all occupied orbitals are strongly bound (lowest IP = 5.4 eV).

is favored by 0.39 eV. Each of these oxygens has two $p\pi$ orbitals perpendicular to the Cu-O-Cu axis, but the $p\pi$ orbital in the plane of structure I is the preferred one for oxidation (by 0.4 eV). This leads to good electrical conduction as discussed below. On the other hand, such a subtle change as replacing part of the La^{3+} with Sr^{2+} can shift the relative ionization potentials (IP) of the apex and sheet oxygens significantly. Thus, with $x = 0.3$, we find that the apex oxygen is preferentially oxidized (by 0.45 eV). We believe that it is subtle shifts in relative IP that lead to a loss in superconductivity above $x = 0.3$ and that this is responsible for the semiconductor character of systems such as $La_4BaCu_5O_{13}$ and $La_5SrCu_6O_{15}$ (which have sheets or chains similar to the 2-1-4 and 1-2-3 systems). Thus, subtle changes in the cations (charges or placement) or in the structure (for example, owing to higher pressure) might change these semiconductors into superconductors.

For the $Y_1Ba_2Cu_3O_{7-y}$ system, there are three types of oxygens, O_C, O_S, and O_B for chain, sheet, and bridge, as indicated in Fig. 1c, but we find a very strong preference for oxidizing the chain oxygens. For $y = 0$, there must be one oxygen hole per central copper and hence an idealized structure would have every bridging O_C oxidized. However, with sufficient positive charge along the chain, it becomes favorable to oxidize sheet oxygens. Holes in O_C can hop easily to adjacent O_C, leading to high mobility if the chain is perfect. Holes in O_S would lead to conduction in the sheets much as in $La_{2-x}Sr_xCu_1O_4$. These two-dimensional sheets should be less sensitive to defects than the chains. Holes in O_B probably serve to communicate between the O_C and O_S sites. Thus, we expect an equilibrium population of holes among O_B, O_C, and O_S, with O_C and O_S important in electrical conduction.

Magnetic coupling in oxidized states. With three singly occupied orbitals, the spins in a Cu^{II}–O^+–Cu^{II} triad can be coupled in three ways ($S = 3/2$ and two $S = 1/2$). Since the singly occupied oxygen $p\pi$ orbital is orthogonal to the Cu^{II} orbitals, there is ferromagnetic coupling between the oxygen $p\pi$ and adjacent copper d orbitals. The spin coupling between the Cu^{II} spins still prefers singlet; however, the Cu-O exchange is much stronger, leading to a ferromagnetic (quartet) ground state. Thus the optimal magnetism of a chain is as in

$$O\text{–}Cu^{II}\uparrow\text{–}O^+\uparrow\text{–}Cu^{II}\uparrow\text{–}O\text{–}Cu^{II}\downarrow\text{–}O \quad \text{(II)}$$

We solved self-consistently for all possible spin states of the various clusters and fitted the results with Eq. 1 to obtain coupling terms of $J_{OCu} = 383$ K, $J_{dd} = -205$ K, and $J^+_{dd} = -139$ K for sheets of $La_{2-x}Sr_xCu_1O_4$, and $J_{OCu} = 405$ K, $J_{dd} = -244$ K, and $J^+_{dd} = -164$ K for chains of $Y_1Ba_2Cu_3O_7$. Here J_{OCu} is for adjacent oxygen $2p$ and copper $3d$ orbitals, J^+_{dd} is for two copper atoms with the intervening oxygen oxidized (the center and left Cu of structure II), and J_{dd} is for a copper pair where the intervening oxygen is not oxidized (the central and right Cu of structure II). Note that the J_{dd} with an intervening O^+ is smaller than that for a normal oxygen (164 K versus 244 K); this is because superexchange decreases when the central atom (oxygen) is less negative (*11*).

In the accompanying report (*12*) it is shown that the interplay between the O-Cu and Cu-Cu magnetic couplings is responsible for the superconductivity in these systems.

Electron correlation. It is important to emphasize that the many-body electron correlations implicit in the GVB wavefunction are essential to a proper description of these clusters (*3*). For example, an ordinary HF calculation on the Cu_2O_7 cluster yields a closed-shell singlet state 6.89 eV above the triplet, while the GVB wavefunction puts the singlet 0.04 eV below the triplet. The problem with the HF description for these systems is that separate singly occupied d orbitals as in Fig. 2, a and b, are not allowed. Thus, for Cu_2O_7, the GVB wavefunction has the form

$$\Psi^{GVB}_{singlet} = \mathcal{A}[\Phi(\phi_L\phi_R + \phi_R\phi_L)(\alpha\beta - \beta\alpha)] \quad (4)$$

where ϕ_L and ϕ_R denote $d_{y^2-z^2}$–like orbitals centered mainly on the left and right copper (as in Fig. 2 for Cu_3), Φ contains all other orbitals and spins, and $\mathcal{A}$ is the antisymmetrizer (determinant operator). All orbitals are calculated self-consistently with no restriction on shape, overlap, or character of the orbitals. Similarly, the triplet state is described as

$$\Psi^{GVB}_{triplet} = \mathcal{A}[\Phi(\phi_L\phi_R - \phi_R\phi_L)(\alpha\beta + \beta\alpha)] \quad (5)$$

where all orbitals are solved for self-consis-

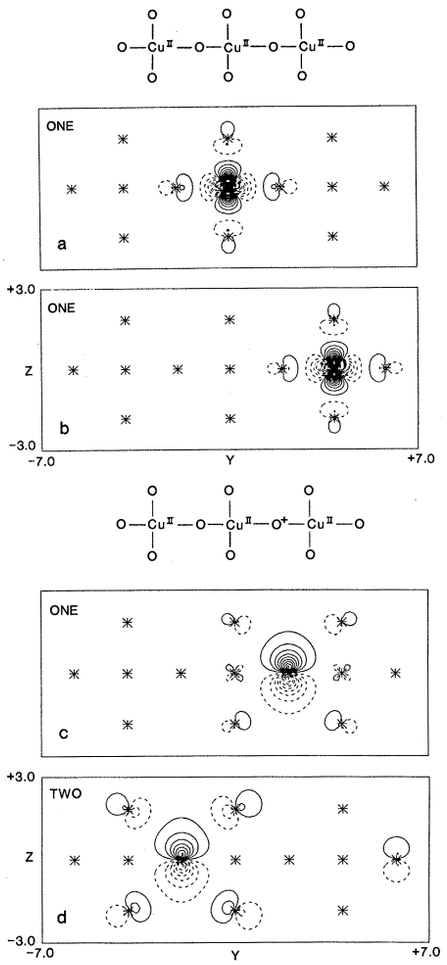

Fig. 2. The GVB orbitals (amplitudes) of Cu_3O_{10} (**a**) and (**b**) show two of the three singly occupied (d-like) orbitals located on the copper centers. Atoms in the plane are indicated with asterisks. Positive contours are solid, whereas negative contours are dotted; the increments are 0.10 atomic units. (**c**) The new singly occupied (oxygen $2p\pi$–like) orbital obtained by ionizing the Cu_3O_{10} cluster. No noticeable change occurs in the other orbitals shown in (a) and (b). (**d**) The corresponding doubly occupied orbital at an adjacent oxygen.

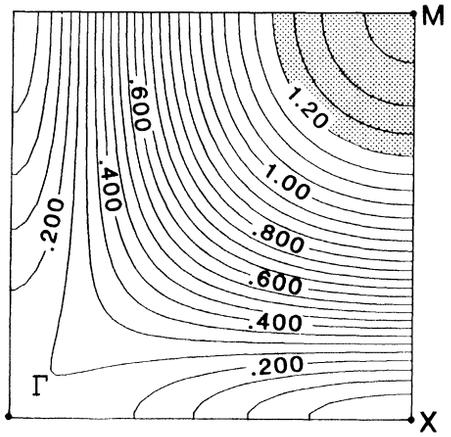

Fig. 3. The upper oxygen $2p\pi$ band for the Cu-O sheets of $La_2Cu_1O_4$ (based on GVB energy band calculations). The contour lines are labeled in electron volts. The Fermi energy for $La_{1.85}Sr_{0.15}Cu_1O_4$ is at the boundary of the dotted and undotted regions.

tently; however, the final orbitals are very similar (indistinguishable in a plot such as Fig. 2) from the optimum orbitals of the singlet. As a result, the Heisenberg-type description (Eq. 1) is suitable. In contrast, the HF functions have the form

$$\Phi^{HF}_{singlet} = \mathcal{A}[\Phi(\phi_g\phi_g)(\alpha\beta - \beta\alpha)] \quad (6)$$

$$\Phi^{HF}_{triplet} = \mathcal{A}[\Phi(\phi_g\phi_u - \phi_u\phi_g)(\alpha\beta + \beta\alpha)] \quad (7)$$

where all orbitals are calculated self-consistently. For the optimum triplet state, the final orbitals have the form

$$\phi_g = (\phi_L + \phi_R) \quad (8)$$

$$\phi_u = (\phi_L - \phi_R) \quad (9)$$

(ignoring normalization), leading to a wavefunction identical to $\Psi^{GVB}_{triplet}$. However, for the singlet state, the HF wavefunction has the form

$$\phi_g\phi_g = (\phi_L\phi_R + \phi_R\phi_L) + (\phi_L\phi_L + \phi_R\phi_R) \quad (10)$$

which includes equal amounts of covalent and ionic character. These ionic terms correspond to equal mixtures of Cu^{III}-Cu^{I} character into the Cu^{II}-Cu^{II} wavefunction, leading to an artificially high energy. This HF wavefunction also leads to strong mixtures between the copper $d\sigma$ and oxygen $p\sigma$ orbitals ($d_{y^2-z^2}$ and p_y in Fig. 2). To remove this difficulty for HF wavefunctions, one can relax the spin symmetry restriction and use a wavefunction of the form

$$\Phi^{UHF} = \mathcal{A}[\Phi(\phi_L\alpha)(\phi_R\beta)] \quad (11)$$

(the unrestricted HF or UHF wavefunction). This leads to much lower energy, but the wavefunction is a mixture of singlet and triplet character and hence one cannot directly obtain parameters for Eq. 1. (The UHF wavefunction leads to singly occupied orbitals that are essentially pure $d_{y^2-z^2}$ in character.) The GVB wavefunction corresponds to converting Eq. 11 into a singlet state (leading to Eq. 4) and then reoptimizing the orbitals self-consistently. In terms of band concepts, the HF description has a half-filled band (ϕ_g occupied and ϕ_u empty), whereas the GVB description has every band orbital half-occupied (ϕ_L and ϕ_R). For the infinite system, localized, singly occupied orbitals such as in Fig. 2 lead to very narrow energy bands. It is well known that such systems are not well described with normal band theory, and an empirical modification (the Hubbard Hamiltonian) is used to obtain UHF-like wavefunctions. For the GVB method, an N-body approach to band calculations is required.

Valence bond band structure—localized versus delocalized states. Consider the Cu_3O_{10} cluster modeling the chains of $Y_1Ba_2Cu_3O_7$. Ionizing this cluster leads to two equivalent localized wavefunctions, Ψ_L and Ψ_R,

Ψ_L O→Cu→O←Cu←O←Cu←O **III**

Ψ_R O→Cu→O→Cu→O←Cu←O **IV**

where structure IV is shown in Fig. 2, c and d. The wavefunction is localized because the shape of a doubly occupied orbital needs to be more expanded (electron repulsion) than that of a singly occupied orbital and because in Ψ_L the other bonds polarize to stabilize a charge on the left, whereas in Ψ_R they polarize to stabilize a charge on the right. These two wavefunctions overlap with a sizeable matrix element between them,

$$\sigma_{LR} = \langle\Psi_L|\Psi_R\rangle = -0.1412 \quad (12)$$

$$H_{LR} = \langle\Psi_L|H|\Psi_R\rangle \quad (13)$$

In the resonating-GVB description of these states, the total wavefunction is written

$$\Psi_u = (\Psi_L + \Psi_R)/\sqrt{1 + S} \quad (14)$$

$$\Psi_g = (\Psi_L + \Psi_R)/\sqrt{1 - S} \quad (15)$$

We calculate these states using the R-GVB program (*13*), which allows every orbital of Ψ_L to overlap every orbital of Ψ_R. This many-electron resonating generalized valence bond (R-GVB) hole description of the ion states is equivalent to a polaron-hopping description in which the hole is completely dressed with polarization for each site. The R-GVB states in structures III and IV lead to a resonance stabilization of 0.33 eV for Ψ_g and destabilization of 0.43 eV for Ψ_u. This leads to a one-dimensional band with bandwidth = 1.62 eV. As a result, holes in the oxygen $2p\pi$ bonds of the Cu-O chains or Cu-O sheets lead to high mobility charge carriers for electrical conductivity.

N-Electron band theory. We report here a band calculations based on such localized N-electron valence bond wavefunctions rather than the traditional one-electron molecular orbitals (MO) or band orbitals. The N-electron band states Ψ_k are described as a linear combination of localized N-electron valence bond wavefunctions,

$$\Psi_k = C_{1k}\Phi_1 + C_{2k}\Phi_2 + \cdots = \sum_i C_{ik}\Phi_i \quad (16)$$

where each term Φ_i is an N-electron wavefunction describing a fully polarized description of the hole on a particular site i. Here the coefficients are calculated by solving

$$\sum_j H_{ij}C_{jk} = \sum_j S_{ij}C_{jk}\lambda_k \quad (17)$$

where the H_{ij} are the N-electron matrix elements (*13*) between oxidized sites i and j and S_{ij} is the N-electron overlap for sites i and j, as in Eqs. 12 and 13. This process is analogous to a tight-binding band calculation except that the matrix elements arise from N-electron valence bond calculations, $\langle\Psi_L|H|\Psi_R\rangle$, where H is the total N-electron Hamiltonian rather than from one-electron matrix elements, $\langle\Phi_L|H^{HF}|\Phi_R\rangle$, where H^{HF} is an effective one-particle Hamiltonian. A wavepacket constructed from the band states, Ψ_k in Eq. 16, describes the motion of a fully dressed polaron.

This contrasts with the tight-binding MO description where the coefficients describe a particular one-electron band orbital

$$\psi_k = C_{1k}\phi_1 + C_{2k}\phi_2 + \cdots = \sum_i C_{ik}\phi_i \quad (18)$$

(in terms of localized atomic-like orbitals ϕ_i), which is occupied along with the other band orbitals to construct a many-electron wavefunction,

$$\Psi^{MO} = \mathcal{A}[(\psi_1)^2(\psi_2)^2\cdots] \quad (19)$$

For the CuO sheets of $La_2Cu_1O_4$, we calculated the valence band shown in Fig. 3. This represents the Bloch N-electron states for a hole moving in the CuO sheets. The most stable ion state is at the M point (highest state in a standard band calculation). The least stable state is the X point. The total bandwidth is 1.38 eV.

For $La_{2-x}Sr_xCu_1O_4$, the maximum transition temperature T_c occurs for $x = 0.15$. Assuming all these holes go into the oxygen $2p\pi$ band leads to the Fermi energy at 0.16 eV below the top of the band, as indicated in Fig. 3. The density of states at the Fermi

energy is $N(0) = 1.14\ eV^{-1}$ per copper atom. For $Y_1Ba_2Cu_3O_7$ the band arising from the chains would be half full if all holes were in this band. This would lead to $N(0) = 0.21\ eV^{-1}$ per chain copper. These results are used in the accompanying report (*12*) to derive the T_c for superconductivity in cuprates.

The Hubbard model. As pointed out above, standard HF methods lead to a very bad description of systems such as these Cu^{II} systems having weakly overlapping orbitals. The result is a strong mixture of the singly occupied $d\sigma$ orbitals ($d_{y^2-z^2}$ pointing from Cu to O) with oxygen $p\sigma$ orbitals, leading to a partially filled band of mixed copper $d\sigma$ and oxygen $p\sigma$ character. With GVB, the electron correlation effects lead to singly occupied $d_{y^2-z^2}$ orbitals on each copper. In terms of band concepts this GVB description corresponds to half occupation of every orbital of the band constructed from $d_{y^2-z^2}$ on each center, whereas HF would start with half occupation of the band. The Hubbard approximation (*14*) to UHF builds in a similar improvement upon standard HF band theory by introducing a repulsive one-center term to split the HF band into up-spin and down-spin bands on separate sublattices (leading to spin waves). The GVB approach treats the electron correlation problem rigorously, leading to pure spin states. However, this leads to the complication that the band states must be calculated in terms of N-body wavefunctions (as presented above) rather than the usual one-particle orbitals.

Several standard one-electron band calculations (based on local density functionals) have been reported (*15*) on $La_2Cu_1O_4$. These band calculations suggest an overall population of d^9 on each copper, in agreement with the GVB results but, as expected, they all involve strong mixing of copper $d\sigma$ and oxygen $p\sigma$ character, leading to a partially occupied band of σ character. A properly parameterized Hubbard Hamiltonian might mimic the GVB results (with the copper $d\sigma$ orbitals forming a narrow band and a highest band that is oxygen $p\pi$–like).

REFERENCES AND NOTES

1. J. G. Bednorz and K. A. Müller, *Z. Phys. B* **64**, 189 (1986); J. M. Tarascon, L. H. Greene, W. R. McKinnon, G. W. Hull, T. H. Geballe, *Science* **235**, 1373 (1987).
2. M. K. Wu, *et al.*, *Phys. Rev. Lett.* **58**, 908 (1987).
3. W. J. Hunt, P. J. Hay, W. A. Goddard III, *J. Chem. Phys.* **57**, 738 (1972); W. A. Goddard III and T. C. McGill, *J. Vac. Sci. Technol.* **16**, 1308 (1979).
4. The geometries of these clusters are based on neutron diffraction data (*5*). The Dunning (9*s*5*p*/3*s*2*p*) double zeta contraction (*6*) of the Huzinaga Gaussian basis set is used for the oxygen atoms. The Los Alamos core effective potential (*7*) is used to replace the 18 core electrons of the copper atom. This leads to a (3*s*,2*p*,2*d*) Gaussian basis for the 11 valence electrons of the copper atom.
5. P. Day *et al.*, *J. Phys. C* **20**, L429 (1987); W. I. F. David *et al.*, *Nature (London)* **327**, 310 (1987).
6. T. H. Dunning, Jr., and P. J. Hay, in *Modern Theoretical Chemistry* (Plenum, New York, 1977), vol. 3, p. 1.
7. P. J. Hay and W. R. Wadt, *J. Chem. Phys.* **82**, 270 (1985).
8. N. D. Mermin and H. Wagner, *Phys. Rev. Lett.* **17**, 1133 (1966).
9. D. Vaknin *et al.*, *ibid.* **58**, 2802 (1987).
10. J. B. Torrance, Y. Tokura, A. Nazzal, S. S. P. Parkin, in preparation; Y. Tokura, J. B. Torrance, A. I. Nazzal, T. C. Huang, C. Ortiz, in preparation.
11. Superexchange involves mixing of charge transfer states (structures VI and VII) into the dominant wavefunction (top structure V diagram). This charge transfer is much less favorable if the oxygen is made more positive.

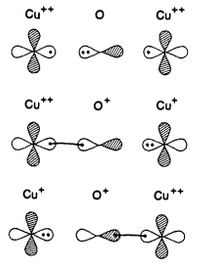

12. G. Chen and W. A. Goddard III, *Science* **239**, 899 (1988).
13. A. F. Voter and W. A. Goddard III, *J. Am. Chem. Soc.* **108**, 2830 (1986). The matrix elements as defined in Eq. 13 would depend on cluster size. We use instead

$$\overline{H}_{ij} = E^{N-1}S_{ij}^{N-1} - H_{ij}^{N-1} \quad (20)$$

where E^{N-1} is the energy of the cluster with one hole, and H_{ij}^{N-1} and S_{ij}^{N-1} are for systems with the hole localized on sites i and j, respectively. The sign chosen in $\overline{H}_{ij}$ is so that $E_k = -IP_k$, where IP_k is the ionization potential out of Bloch state k, leading to band diagrams analogous to one-electron band diagrams.
14. J. Hubbard, *Proc. R. Soc. London Ser. A.* **281**, 401 (1964).
15. L. F. Mattheiss, *Phys. Rev. Lett.* **58**, 1028 (1987); K. Takegahara, H. Harima, A. Yanase, *Jpn. J. Appl. Phys.* **26**, L352 (1987); T. Oguchi, *ibid.*, p. L417.

16. We thank the Office of Naval Research and the donors of the Petroleum Research Fund (administered by the American Chemical Society) for partial support of this research. We thank C. M. Kao and G. Chen for assistance and useful discussions. The GVB and R-GVB calculations were carried out on the Alliant FX8/8 and DEC VAX 8650 computers in the Caltech Materials Simulation Facility [funded by the National Science Foundation–Materials Research Groups (grant DMR-84-21119); the Office of Naval Research/Defense Advanced Research Projects Agency (contract N00014-86-K-0735); the Department of Energy–Energy Conversion and Utilization Technology (JPL code 49-242-E0403-0-3550), the National Science Foundation–Chemistry (grant CHE-8318041), and the Office of Naval Research (contract N00014-84-K-0637)].

7 December 1987; accepted 20 January 1988

The Magnon Pairing Mechanism of Superconductivity in Cuprate Ceramics

GUANHUA CHEN AND WILLIAM A. GODDARD III

The magnon pairing mechanism is derived to explain the high-temperature superconductivity of both the $La_{2-x}Sr_xCu_1O_4$ and $Y_1Ba_2Cu_3O_7$ systems. Critical features include (i) a one- or two-dimensional lattice of linear Cu-O-Cu bonds that contribute to large antiferromagnetic (superexchange) coupling of the Cu^{II} (d^9) orbitals; (ii) holes in the oxygen $p\pi$ bands [rather than Cu^{III} (d^8)] leading to high mobility hole conduction; and (iii) strong ferromagnetic coupling between oxygen $p\pi$ holes and adjacent Cu^{II} (d^9) electrons. The ferromagnetic coupling of the conduction electrons with copper d spins induces the attractive interaction responsible for the superconductivity, leading to triplet-coupled pairs called "tripgems." The disordered Heisenberg lattice of antiferromagnetically coupled copper d spins serves a role analogous to the phonons in a conventional system. This leads to a maximum transition temperature of about 200 K. For $La_{1.85}Sr_{0.15}Cu_1O_4$, the energy gap is in excellent agreement with experiment. For $Y_1Ba_2Cu_3O_7$, we find that both the CuO sheets and the CuO chains can contribute to the supercurrent.

THE EXCITING DISCOVERIES FIRST of the 2-1-4 class of high-temperature superconductors (*1*) (best is, $La_{2-x}Sr_xCu_1O_4$ with transition temperature $T_c = 40$ K) and then of the much higher temperature 1-2-3 system (*2*) ($Y_1Ba_2Cu_3O_7$ with $T_c = 93$ K) have led to a frenzied chase after even higher temperature superconductors and more easily processed materials. Simultaneously, the theoretical community has struggled with how to understand the origin of the superconductivity in these conducting ceramics. The need for such a theory is reinforced by the lack of any substantial increase in T_c, despite an enormous effort by materials scientists around the world (*3*). The problem has been the lack of a theoretical framework within which one could reason about the likely effects of various changes in composition or structure. We propose here such a model.

Recent calculations (*4*) indicate that the $La_{2-x}Sr_xCu_1O_4$ and $Y_1Ba_2Cu_3O_7$ classes of

Arthur Amos Noyes Laboratory of Chemical Physics, California Institute of Technology, Pasadena, CA 91125.